Chemie der Erde 78 (2018) 372–384

Contents lists available at ScienceDirect

Chemie der Erde

journal homepage: www.elsevier.com/locate/chemer

New constraints on elemental and Pb and Nd isotope compositions of South American and Southern African aerosol sources to the South Atlantic Ocean

R. Khondoker[a], D. Weiss[a,*], T. van de Flierdt[a], M. Rehkämper[a], K. Kreissig[a], B.J. Coles[a], S. Strekopytov[b], E. Humphreys-Williams[b], S. Dong[a,c], A. Bory[d], V. Bout-Roumazeilles[d], P. Smichowski[e], P. Cid-Agüero[f], M. Babinski[g], R. Losno[h], F. Monna[i]

[a] Dept. of Earth Science & Engineering, Imperial College London, SW7 2AZ, UK
[b] Natural History Museum, London, SW7 5BD, UK
[c] CRPG, UMR-CNRS 7358, Vandœuvre les Nancy, France
[d] University of Lille, CNRS, University of Littoral Côte d'Opale, UMR 8187, LOG, Laboratoire d'Orceanologie et de Géosciences, F 59000 Lille, France
[e] National Atomic Energy Commission, Av. Gral Paz 1499, Buenos Aires, Argentina
[f] University of Magallanes, Avda. Bulnes, 01855, Punta Arenas, Chile
[g] Geochronological Research Centre, University of São Paulo, São Paulo, Brazil
[h] LISA Faculty of Science, University of Paris, Batiment P4 393, Paris, France
[i] Univerisity of Bourgogne, Batiment Gabriel, Dijon, France

ARTICLE INFO

Handling Editor: Dewashish Upadhyay

Keywords:
Isotopic and elemental composition
Source characterisation
Geochemical assessment
Aerosol
South America
Southern Africa
South Atlantic Ocean

ABSTRACT

Improving the geochemical database available for characterising potential natural and anthropogenic aerosol sources from South America and Southern Africa is a critical precondition for studies aimed at understanding trace metal controls on the marine biogeochemical cycles of the South Atlantic Ocean. We here present new elemental and isotopic data for a wide range of sample types from South America and Southern Africa that are potentially important aerosol sources. This includes road dust from Buenos Aires and lichen samples from Johannesburg, soil dust from Patagonia, volcanic ash from the Andean volcanic belt, and aerosol samples from São Paulo. All samples were investigated for major (Al, Ca, Fe, Mg, Na, K, Mn) and trace element (Cd, Co, Cr, Cu, Ni, Pb, REE, Sc, Th, Y, V, Zn) concentrations and Nd and Pb isotopic compositions. We show that diagrams of $^{208}Pb/^{207}Pb$ vs. ε_{Nd}, $^{208}Pb/^{207}Pb$ vs. Pb/Al, 1/[Pb], Zn/Al, Cd/Al, Cu/Al, and ε_{Nd} vs. Pb/Al, and 1/[Nd] are best suited to separate South American and South African source regions as well as natural and anthropogenic sources. A subset of samples from Patagonia and the Andes was additionally subjected to separation of a fine (< 5 μm) fraction and compared to the composition of the bulk sample. We show that differences in the geochemical signature of bulk samples between individual regions and source types are significantly larger than between grain sizes. Jointly, these findings present an important step forward towards a quantitative assessment of aeolian trace metal inputs to the South Atlantic Ocean.

1. Introduction

The atmosphere is a major pathway for delivering elements essential for primary production to surface waters (e.g., Boyd et al., 2000; Mahowald et al., 2005). Understanding the origin of aerosols that reach the ocean is a key challenge for deciphering marine biogeochemical processes and their possible impact on the global carbon cycle and on the climate system (Morel et al., 2003; Mahowald et al., 2005). A geographical area of particular interest is the South Atlantic, where the source of nutrient supply has been discussed (e.g., Boyd et al., 2000; Galloway et al., 2004; Mahowald et al., 2005; Meskhidze et al., 2007; Li et al., 2008), and where global dust models yield estimates on the flux of nutrients that differ significantly (e.g., Prospero et al., 2002; Mahowald et al., 2005, 2009; Gasso and Stein, 2007; Johnson et al., 2010).

Atmospheric modelling and satellite mapping indicate that Patagonia and the Puno-west Argentinian region are the main natural dust sources from South America to supply aerosols to the South Atlantic Ocean (Prospero et al., 2002; Gasso and Stein, 2007). Large arid regions such as the Namib, Sossusvlei and Kalahari deserts in South Africa are major dust sources on the other side of the South Atlantic (Chin, 2009). Due to the prevailing wind direction of the westerlies they

* Corresponding author.
E-mail address: d.weiss@imperial.ac.uk (D. Weiss).

https://doi.org/10.1016/j.chemer.2018.05.001
Received 15 August 2016; Received in revised form 18 July 2017; Accepted 24 May 2018

however only deliver aerosols to the more proximal areas of the South Atlantic (Piketh, 2002). Meanwhile, a study of geochemical characteristics of aerosols over the South Atlantic Ocean (Witt et al., 2006) revealed trace metal enrichment relative to the continental crust, associated with air mass back trajectories passing from South America towards the South Atlantic. The data suggest a significant imprint of South American anthropogenic sources on aerosols arriving at the ocean (Witt et al., 2006). Dissolution studies furthermore imply that anthropogenic aerosols typically release elements more readily into seawater than natural particles (e.g., Spokes et al., 1994; Ebert and Baechmann, 1998; Desboeufs et al., 2001; Sholkovitz et al., 2009; Hsu et al., 2010), an observation with far reaching implications for ocean biogeochemical cycles.

One way to distinguish natural and anthropogenic particulate contributions in aerosols is by examining their geochemical fingerprint alongside that of potential source regions (e.g., Bollhöfer and Rosman, 2000; Monna et al., 2006; Gioia et al., 2010; Fujiwara et al., 2011). Variations in elemental and isotopic compositions of different source rock formations allows for source characterisation and thus provenance assessment of aerosols (e.g., Gaiero et al., 2003, 2004; Ferrat et al., 2011). For example, Pb isotopes are useful provenance indicators due to radioactive decay of ^{232}Th to ^{208}Pb, ^{235}U to ^{207}Pb and ^{238}U to ^{206}Pb (e.g. Bollhöfer and Rosman, 2000; Gioia et al., 2010). It has been shown that individual Pb-ore bodies carry distinct isotopic compositions depending on age and initial Th and U content of the source rock. This in turn allows depicting anthropogenic sources, which emit Pb from different ore bodies (e.g., Bollhöfer and Rosman, 2000 and 2001). Neodymium isotopes, on the other hand, are widely applied to distinguish between natural sources exploiting the ^{147}Sm-^{143}Nd decay system. The Nd isotopic compositions are typically expressed as ε_{Nd} values, which denote the deviation of the ^{143}Nd/^{144}Nd ratio of a rock from the bulk earth value in parts per 10,000 (Jacobsen and Wasserburg, 1980). Younger, mantle-derived rocks are thereby characterised by positive ε_{Nd}, whilst older, crustal rocks are characterised by negative ε_{Nd} values.

Numerous studies investigated the elemental and isotopic compositions of natural sources, such as loess, volcanic deposits, and other rock formations, from the Andes and Patagonia in South America (e.g., Gaiero et al., 2003, 2004, 2007; GEOROC et al., 2003–2011GEOROC, 2018GEOROC et al., 2003–2011; Delmonte et al., 2004; Sugden et al., 2009) and desert, ore deposit and volcanic regions across Southern Africa (e.g., Condie and Hunter, 1976; Le Roex and Lanyon, 1998; Janney et al., 2002; Le Roex et al., 2003; Ewart et al., 2004; Delmonte et al., 2004; GEOROC et al., 2003–2011GEOROC, 2018GEOROC et al., 2003–2011). In contrast, fewer studies on elemental or isotopic compositions of anthropogenic aerosol sources from South America and Southern Africa have been conducted, resulting in limited data availability (e.g., Bollhöfer and Rosman, 2000; Babinski et al., 2003; Monna et al., 2006; Gioia et al., 2010; Gioia et al., 2017; Fujiwara et al., 2011).

This study aims to extend the geochemical characterisation of potential natural and anthropogenic aerosol sources from South America and Southern Africa. A large range of samples were analysed for major and trace element concentrations, as well as for Pb and Nd isotope compositions. In detail, our study provides new data for road dust from Buenos Aires, lichen and tree bark from Johannesburg, additional bulk samples from Patagonia (mineral dust), the Andean Volcanic Belt (volcanic deposits), and São Paulo (urban aerosols). Moreover, we analysed the fine grain size fraction (< 5 μm) of selected bulk samples (samples that have not been particle size separated and include all gran sizes present at sampling site) to assess the importance of particle size for geochemical source characterisation (Raes et al., 2000; Chang et al., 2000; Honda et al., 2004; Feng et al., 2010; Ferrat et al., 2011). We use our new data, in conjunction with previously published results, to identify a suite of geochemical parameters, which are best suited to distinguish potential aerosol sources to the South Atlantic.

2. Methods

2.1. Study area

Fig. 1 shows simplified geological maps of relevant potential source areas for aerosols in South America and Southern Africa. South America can be divided into the northern and central Archean/Neoproterozoic shield area, known as the South American Platform, the Phanerozoic covers of the Patagonian plateau, and the Andean volcanic fold belt and sedimentary basins along the western margin of the continent. The South American Platform is composed of metamorphic rocks in amphibolite to granulite facies and igneous, granitic complexes. It is constrained by volcanic and sedimentary formations along the eastern margin resulting from the Brasiliano/Pan African extension (Almeida et al., 2000; Brito Neves and Fuck, 2013). Patagonia is dominated by volcanic rocks (basalts, andesites, rhyolites) and plutons, as well as sediment that overlies a granitic basement of Mesozoic age (Almeida et al., 2000; Alkmim et al., 2001; Ducart et al., 2006; Rosello et al., 2008; Marfil and Maiza, 2012; Brito Neves and Fuck, 2013). The Andes can be subdivided into four volcanic zones: the northern volcanic zone (NVZ; > 10°S), central volcanic zone (CVZ; 10–34°S), southern volcanic zone (SVZ; 32–40°S) and austral volcanic zone (AVZ; 40–52°S). They are composed of Cenozoic volcanism of silicic composition, intermediate to basic lava flows along a volcanic arc to the west, and basaltic back arc lava flows across the east (Jakes and White, 1972; Dostal et al., 1977; Grunder, 1987; Rapela and Kay, 1988; Kay et al., 2006; Stern and Kilian, 1996).

Southern Africa is largely composed of an Archean to Neoproterozoic shield of intermediate to basic volcanic and metamorphic formations (Condie and Hunter, 1976; Le Roex et al., 2003; Begg et al., 2009; Fig. 1). Phanerozoic covers (typically mafic, olivine basaltic lava flows and sedimentary basins) characterise the area to the south of the shield, across the southern coastline of South Africa and along the coastline of Namibia (Le Roex and Lanyon, 1998; Ewart et al., 2004; Janney et al., 2002; Begg et al., 2009).

2.2. Sampling strategy and sample descriptions

The locations of samples selected for this study are shown in Table 1 and Fig. 1 alongside additional relevant samples from the literature. Also highlighted are samples from Buenos Aires and Johannesburg that were previously analysed for elemental or isotopic compositions.

Topsoil and riverbed sediments were collected in southern Patagonia in 2012 from Rio Santa Cruz, Bahia San Sebastian, Rio Gallegos, El Calafate and Punta Arenas National Parks (34–55°S) to represent potential mineral dust sources from Patagonia. Volcanic tephra and clast deposits were collected from the volcanic slopes of Chaiten volcano in 2008 and the Puyehue volcano in 2011, to characterise the southern volcanic zone of Patagonia. Note that some of our results on the Chaiten volcano have also been reported by. One volcanic topsoil sample was obtained from Cotopaxi volcano in the northern volcanic zone in 2010, to cover a potential source area that may impact the South Atlantic during unusual atmospheric circulation patterns or large volcanic eruptions.

Size fraction samples (50–75 μm, and 75–100 μm) of road dusts were collected in Buenos Aires between 2006 and 2007, to characterise an important potential source for urban aerosols (Fujiwara et al., 2011). A dustpan and brush were used to collect dust at pavement edges that accumulated over a two-month period, covering an area of about 7 × 12 km. Following collection, samples were sieved to remove large debris, such as leaves and brick, dried at 100 °C for 24 h and then sieved again. The samples were obtained from urban zones with different traffic patterns and urban characteristics, but were not collected adjacent to site-specific pollution sources.

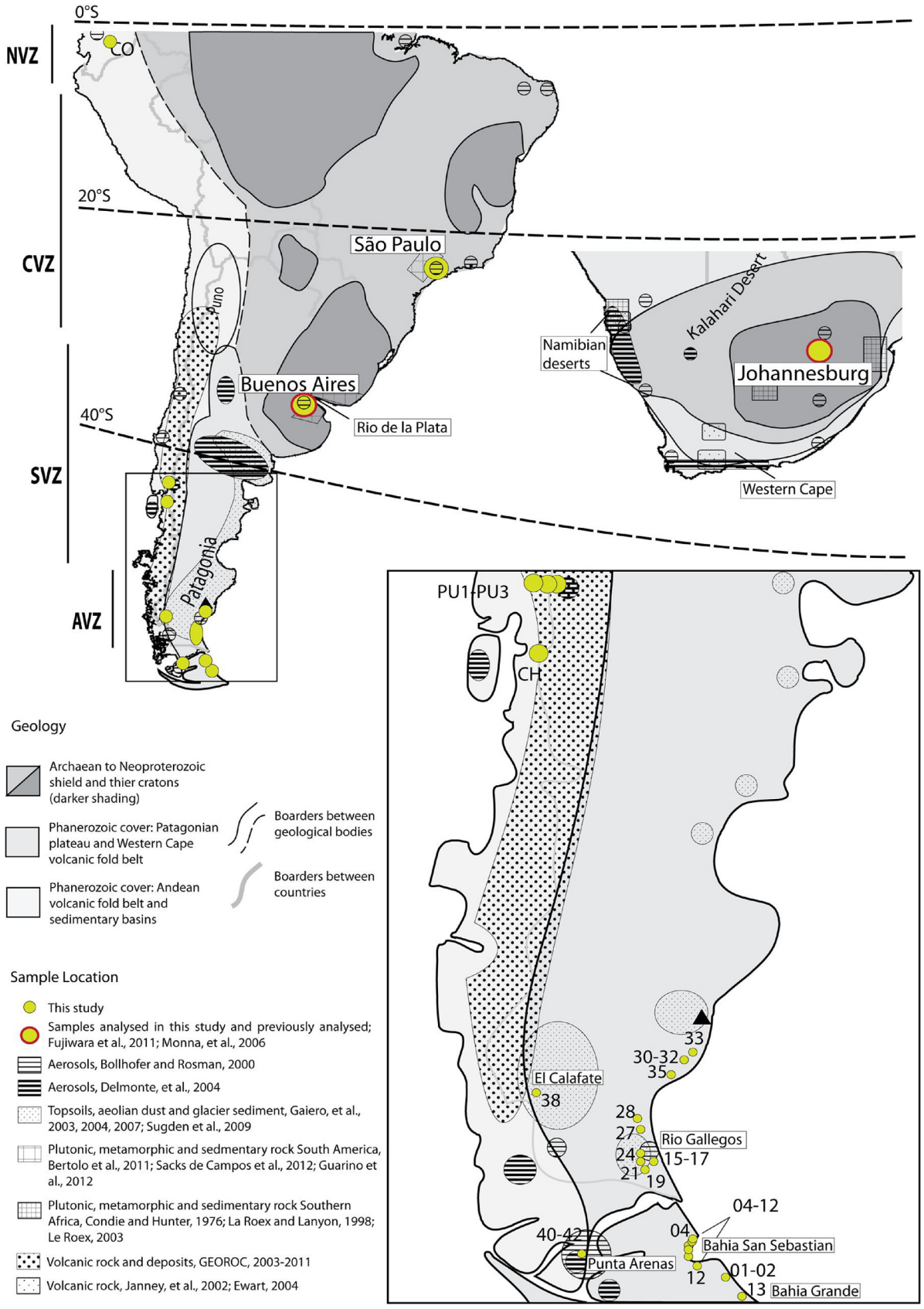

Fig. 1. Map showing the location of samples analysed in this study and the literature. Also shown are basic geological formations in South America (taken from Almeida et al., 2000, and Brito Neves and Fuck, 2013) and Southern Africa (taken from Tohver et al., 2006, and Begg et al., 2009).

Table 1
Sample location and sample types from South America and Southern Africa.

Sample ID	Sample Location	Sample Type	Longitude (°)	Latitude (°)
South America				
Argentina				
Bulk				
4[a]	Bahia San Sebastian, Southern Patagonia	Topsoil	−68.39	−52.99
5	Bahia San Sebastian, Southern Patagonia	Topsoil	−68.39	−53.04
8	Bahia San Sebastian, Southern Patagonia	Topsoil	−68.50	−53.14
9	Bahia San Sebastian, Southern Patagonia	Topsoil	−68.57	−53.17
10	Bahia San Sebastian, Southern Patagonia	Topsoil	−68.57	−53.20
11	Bahia San Sebastian, Southern Patagonia	Topsoil	−68.57	−53.23
12	Bahia San Sebastian, Southern Patagonia	Topsoil	−68.52	−53.32
19	Rio Gallegos, Southern Patagonia	Topsoil	−69.53	−51.81
21	Rio Gallegos, Southern Patagonia	Topsoil	−69.60	−51.71
35	Rio Santa Cruz, Southern Patagonia	Topsoil	−68.94	−50.24
40	Punta Arenas, Southern Patagonia	Topsoil	−71.11	−53.29
42[a]	Punta Arenas, Southern Patagonia	Topsoil	−71.11	−53.29
1	Rio Grande, Southern Patagonia	Lagoon sediment	−68.07	−53.59
2	Rio Grande, Southern Patagonia	Lagoon sediment	−68.07	−53.59
13	Rio Grande, Southern Patagonia	Topsoil/Bed sediment	−67.80	−53.83
15	Rio Grande, Southern Patagonia	Topsoil/Bed sediment	−69.28	−51.73
17	Rio Grande, Southern Patagonia	Topsoil/Bed sediment	−69.28	−51.73
24	Rio Grande, Southern Patagonia	Topsoil/Bed sediment	−69.64	−51.63
27	Bahia Grande, Southern Patagonia	Topsoil/Bed sediment	−69.51	−51.16
28	Bahia Grande, Southern Patagonia	Topsoil/Bed sediment	−69.53	−51.09
30	Rio Santa Cruz, Southern Patagonia	Bed Sediment	−68.90	−49.97
32[a]	Rio Santa Cruz, Southern Patagonia	Bed Sediment	−68.90	−49.97
33	Rio Santa Cruz, Southern Patagonia	Bed Sediment	−68.56	−49.83
38	Argentino Lake, Southern Patagonia	Bed Sediment	−72.17	−50.31
50–75 μm				
3C	Urban Area, Buenos Aires	Road dust	−58.51	−34.60
9C	Urban Area, Buenos Aires	Road dust	−58.48	−34.59
110C	Urban Area, Buenos Aires	Road dust	−58.49	−34.65
112C	Urban Area, Buenos Aires	Road dust	−58.49	−34.65
75–100 μm				
3D	Urban Area, Buenos Aires	Road dust	−58.51	−34.60
9D	Urban Area, Buenos Aires	Road dust	−58.48	−34.59
110D	Urban Area, Buenos Aires	Road dust	−58.49	−34.65
112D	Urban Area, Buenos Aires	Road dust	−58.49	−34.65

Sample ID	Sample Location	Sample Type	Longitude (°)	Latitude (°)
Brazil				
< 10 μm				
631	Urban Area, São Paulo	Aerosol	−46.72	−23.56
648	Urban Area, São Paulo	Aerosol	−46.72	−23.56
649	Urban Area, São Paulo	Aerosol	−46.72	−23.56
650	Urban Area, São Paulo	Aerosol	−46.72	−23.56
660	Urban Area, São Paulo	Aerosol	−46.72	−23.56
665	Urban Area, São Paulo	Aerosol	−46.72	−23.56
Chile				
Bulk				
CH[a]	Chaiten Volcano, Southern Volcanic Zone	Volcanic tephra	−71.03	−43.02
PU1	Puyehue Volcano, Southern Volcanic Zone	Volcanic tephra	−71.16	−40.62
PU2[a]	Puyehue Volcano, Southern Volcanic Zone	Volcanic tephra	−71.16	−41.06
PU3	Puyehue Volcano, lakeside near La Angostura	Volcanic clast deposits	−71.64	−40.76
Ecuador				
Bulk				
CO	Cotopaxi Volcano, Northern Volcanic Zone	Volcanic topsoil	−78.44	−0.68
Southern Africa				
South Africa				
Bulk				
PILA	Rural Area, Johannesburg	Lichen	28.00	−26.00
Bulk				
RIV	Urban Area, Johannesburg	Lichen	28.06	−26.06
DEL	Urban Area, Johannesburg	Lichen	28.00	−26.00
CMG	Urban Area, Johannesburg	Lichen	28.03	−26.20
EMER	Urban Area, Johannesburg	Lichen	28.01	−26.16
HUDD	Urban Area, Johannesburg	Lichen	28.11	−26.11
BOT2	Urban Area, Johannesburg	Lichen	27.99	−26.15
Bulk				
DRD-TB	Mine Dump Site, Johannesburg	Tree bark	27.88	−26.18

[a] denotes samples that were analysed for the < 5 μm particle size assessment; bulk samples are samples that have not been particle size separated.

Aerosol samples (PM_{10}) from São Paulo were selected to characterise emissions from an additional urban environment. These aerosol samples were collected at the University of São Paulo over a four-day period in the winter of 2005 using methods described in detail in Babinski et al. (2003). The sampling area was located 500 m south of a beltway with intense traffic. Stacked filter units were used to collect aerosol on 47 mm diameter Teflon membranes, during 24 h, sampling a < 10 µm aerosol fraction, with an airflow rate of ~ 16 l min^{-1}.

The lichen and tree bark were collected in Johannesburg between 2001 and 2003, to characterise potential aerosols originating from South Africa (Monna et al., 2006). Five lichen samples are from urban areas, one lichen is from a rural area, whilst the single tree bark sample was collected adjacent to a mine dump site. Details of the sampling locations and methods are given in Monna et al. (2006). In brief, lichen growing on trees was collected between 1 and 3 m above ground level by means of pre-cleaned plastic knives. In the lab, remaining leaf debris were removed and the samples dried at 80 °C over a period of 2 days.

2.3. Sample digestion

Fifty milligrams of bulk topsoil, riverbed sediment, and volcanic samples were weighed into 14.7 ml screw top Savillex PTFE vessels and digested on a hotplate for 48 h in a mixture of 1 ml concentrated HF (30 M) and 0.25 ml concentrated HNO_3 (15.6 M) at 120 °C with daily ultrasonication following the digestion method of Yu et al. (2001). Samples were then evaporated to dryness and re-fluxed twice in 0.5 ml 15.6 M HNO_3 to dissolve any solid fluorides that may have formed due to excess HF, as insoluble fluorides will affect the recovery of the rare earth elements (REEs) and other trace metals.

Aerosol filters from São Paulo (half a circular Teflon filter; 4.7 cm in diameter) were acid washed with 5 ml 15.6 M HNO_3 at 120 °C for 24 h in 14.7 ml screw top Savillex PTFE vessels to remove particulates. Following evaporation, these samples were then digested using the hotplate digestion procedure described above.

Fifty milligrams of lichen and tree bark from Johannesburg were weighed into 14.7 ml screw top Savillex PTFE vessels and treated with a mixture of 2 ml concentrated $HClO_4$ (11 M) and 1 ml 15.6 M HNO_3 on a hotplate for 1–3 h at 90 °C, then 1 h each at 110 °C, 140 °C, 180 °C and 220 °C in order to break down organics. The Savillex vials were uncapped throughout this procedure. Following this initial step, the samples were evaporated to dryness and then underwent the same HF/HNO_3 digestion procedure described above.

After digestion, all samples were taken up in nitric acid to obtain ~ 4 ml of sample solution in ~ 0.8 M HNO_3. From this solution, 1.5 ml were taken for Pb and Nd isotope ratio measurements, 1.5 ml for determination of elemental concentrations and 1 ml were archived. The concentration aliquot was further diluted to 5 ml ~ 0.8 M HNO_3 prior to analysis.

2.4. Elemental analysis

Major (Al, Ca, Fe, Mg, Na, K, Mn) and some trace element (Cd, Co, Cr, Cu, Ni, Pb, V, Zn) concentrations were determined by inductively coupled plasma atomic emission spectroscopy (ICP-AES) using a Thermo iCap 6500 Duo at the Natural History Museum (NHM) in London. Scandium, Th, Y, and REE concentrations were determined by quadrupole inductively coupled plasma mass spectrometry (ICP-MS) using an Agilent 7700 x instrument at the NHM. Detection limits for all elements were calculated after each run based on the signal intensity and standard deviation measurements of the calibration blank relative to a calibration standard and were at or below the ng ml^{-1} level for all elements studied (see Supplementary Table S1). Procedural blank solutions were prepared with similar acid mixtures and under identical experimental conditions as the source samples and yielded concentrations below detection limits for all elements of interest. Supplementary Table S2 and S3 show the major, trace and rare earth elemental concentration data.

Data quality, including total dissolution of samples, was monitored with the reference material USGS G-2 granite (n = 12). The concentration data for G-2 are listed in supplementary Tables S2 and S3 alongside the results for samples. The reproducibility (expressed as ± 1 RSD, relative standard deviation) was better than 5% for major elements, better than 3% for REEs, and better than 8% for other trace elements except Cd (< 23%) and Yb (< 13%). As the G-2 granite contains refractory phases, the results provide a measure for the maximum uncertainty introduced by sample digestion.

2.5. Lead and Nd isotope analysis

Lead was isolated from the sample matrix by ion exchange chromatography using Eichrom Sr spec resin (Weiss et al., 2004). Neodymium was isolated using a two-step column procedure (Pin and Zalduegui, 1997). The REE fraction was separated from the sample matrix using Eichrom TRU spec resin, followed by isolation of the Nd fraction from the other REEs using Eichrom Ln spec resin on volumetrically calibrated Teflon columns. Lead and Nd isotopic compositions were analysed on a Nu Plasma (Nu Instruments Limited, UK) MC-ICP-MS (multiple collector inductively coupled plasma mass spectrometer) instrument, to which samples were introduced with a DSN-100 Desolvation Nebulizer System and a PTFE nebulizer.

For Pb isotope analysis, samples and NIST SRM 981 Pb standards were doped with NIST SRM 997 Tl to a Pb/Tl ratio of 3:1 for correction of the instrumental mass bias using the technique of external normalisation (Weiss et al., 2004). The precision and accuracy of the Pb isotope measurements were assessed using reference material USGS G-2 granite. Over a five-month period, repeated analyses yielded the following ratios and associated 2sd uncertainties: $^{206}Pb/^{204}Pb = 18.399 \pm 0.016$, $^{207}Pb/^{204}Pb = 15.640 \pm 0.014$, and $^{208}Pb/^{204}Pb = 38.902 \pm 0.044$ (n = 22). These results for USGS G-2 are in agreement with published data (18.396 ± 0.023, 15.636 ± 0.005, 38.900 ± 0.019, respectively, Weis et al., 2006). Procedural blanks were negligible at < 50 pg.

For Nd isotope analysis, samples and the JNdi-1 Nd isotope standard were corrected for mass fractionation by normalising to $^{146}Nd/^{144}Nd = 0.7219$. Repeated analysis of the JNdi-1 yielded $^{143}Nd/^{144}Nd$ ratios of 0.512147 ± 0.000016 (n = 26). All sample results were normalised to the recommended value of 0.512115 ± 0.000007 (Tanaka et al., 2000). Repeated analyses of the USGS G-2 granite (n = 22) yielded $^{143}Nd/^{144}Nd$ ratios of 0.512230 ± 0.000025, in agreement with literature results ($^{143}Nd/^{144}Nd = 0.512235 \pm 0.000015$; Weis et al., 2006). Neodymium blanks were negligible at < 10 pg.

Lead and Nd isotopic compositions of the samples and the G-2 reference material are listed in supplementary Table S4.

2.6. Separation of a < 5 µm diameter particle size fraction from South American topsoils and riverbed sediments

A fine fraction (< 5 µm diameter) was separated from three topsoils and riverbed sediments collected from Rio Gallegos, Bahia San Sebastian and Punta Arenas in southern Patagonia, and two volcanic tephra samples from the Chaiten and Puyehue volcanoes in the Andean volcanic belt, within western Patagonia (marked with an asterix in Table 1).

Bulk samples were wet sieved with ultraclean (MQ) water through 60 µm nylon mesh into 90 ml Savillex beakers. The supernatant was siphoned off from the < 60 µm fraction using acid cleaned pipettes. The < 60 µm fraction was then transferred to 15 ml centrifuge tubes, 10 ml of MQ water was added, and samples were shaken with a vortex shaker and left to stand for 45 min to allow for gravimetric separation of the < 5 µm fraction. In water of 20 °C, a 5 µm diameter particle settles by 10 cm every 1.5 h, or by 5 cm in 45 min. The top 5 ml

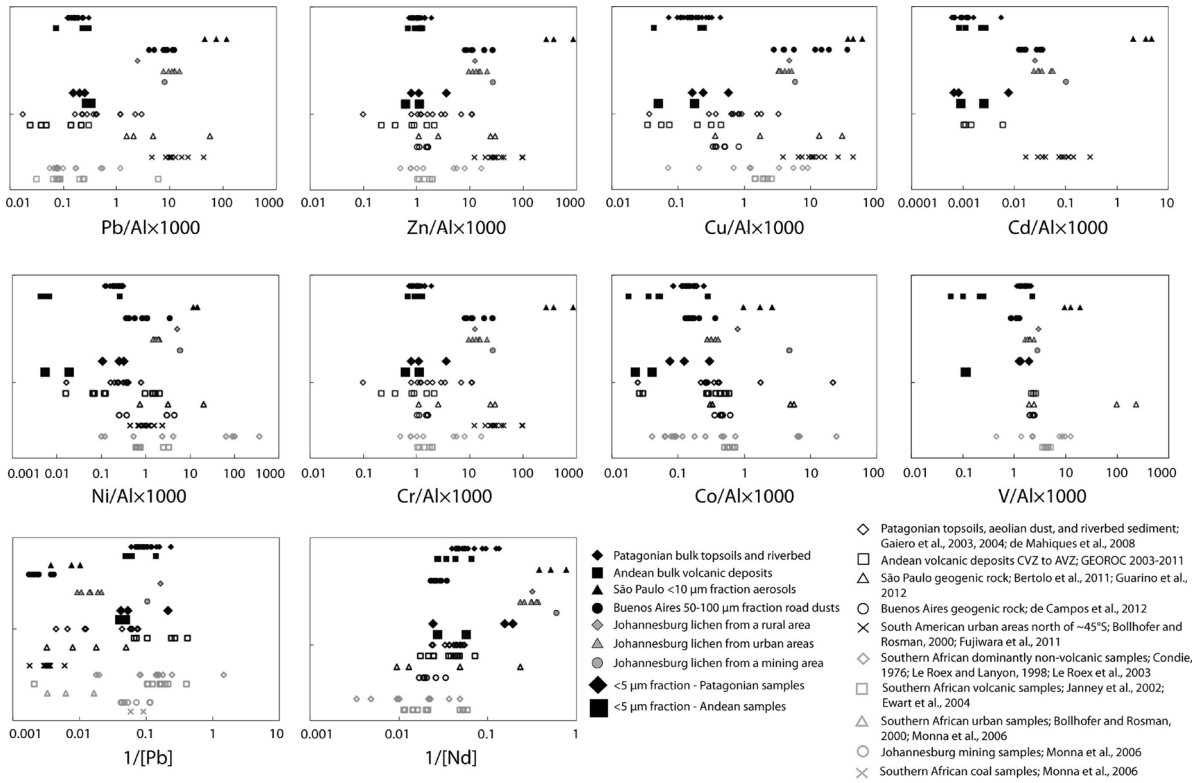

Fig. 2. Selected trace element/Al ratios, and 1/[Pb], 1/[Nd] data for samples from this study (filled symbols) and the literature (open symbols). All measurement uncertainties are smaller than the size of the symbols.

containing the < 5 µm fraction was subsequently siphoned into a separate 15 ml centrifuge tube. The < 60 µm fraction was re-filled with MQ to 10 ml, shaken and left to stand for 45 min. This step was repeated by up to 4 times until the complete < 5 µm fraction was removed from the < 60 µm fraction. The < 5 µm fraction was then centrifuged for 45 min, the supernatant was removed, and the fine fraction sediment was left to dry in a laminar flow hood. The resulting < 5 µm fractions were digested and processed following the methods described in Sections 2.3–2.5.

The elemental concentrations and isotope compositions determined for the < 5 µm fine fraction samples are listed in supplementary Tables S2 to S4.

3. Results and discussion

3.1. Geochemical characteristics of the sources

Following a detailed regression analysis of all available data (Tables S2 to S4), a number of element and isotope ratios were empirically identified as providing the best available parameters for characterising the various distinct source regions and types of aerosols. In detail, these are, Pb/Al, Zn/Al, Cu/Al, Cd/Al, V/Al, Ni/Al, Cr/Al, Co/Al, 1/[Pb], 1/[Nd], and $^{206}Pb/^{207}Pb$, $^{208}Pb/^{207}Pb$ and ε_{Nd} (see Fig. 2).

3.1.1. Patagonian top-soils and riverbed sediments

Trace element/Al ratios are low in the sediments from Patagonia, e.g., Pb/Al × 1000 ratios range from 0.1 to 0.3 and Zn/Al × 1000 ranges from 0.8 to 2. These results fall within the range of previously reported dust, topsoil, and riverbed sediment from across Patagonia (Gaiero et al., 2003, 2004; Fig. 2), suggesting that the samples are representative of natural mineral dust sources from within Patagonia. The elemental compositions are, however, more homogenous than previously analysed samples from this region (Gaiero et al., 2003, 2004), most likely due to the smaller geographical coverage. The 1/[Pb] and 1/[Nd] ratios and Pb and Nd isotope compositions expand beyond the data ranges of previous studies (Figs. 2 and 3; Gaiero et al., 2003, 2004; Gaiero et al., 2007; Mahiques et al., 2008), which suggests that our new results may be of value for defining the compositional endmembers of Patagonian dust sources. The Pb and Nd isotopic compositions are in accord with the young age of the Patagonian range (Fig. 3).

To our knowledge, no Cd data have been previously reported for sediments from Patagonia. Our new results show very low Cd/Al × 1000 ratios, in the range of 0.0007–0.006 (Fig. 2). Such ratios may be a key elemental characteristic of loess samples from Patagonia and may reflect Cd removal by aqueous processes (e.g., Prokop et al., 2003).

3.1.2. Andean volcanic deposits

The volcanic deposits from the NVZ and SVZ show similar and low trace element/Al ratios as well as radiogenic isotopic compositions relative to previously reported data for basaltic to andesitic volcanic rocks from across the CVZ to AVZ (GEOROC, 2003–2011GEOROC, 2018GEOROC, 2003–2011; Gaiero et al., 2003, 2004, 2007; Figs. 2 and 3). The isotopic results are in accord with the young age of the volcanic deposits along the Andean belt. All assessed elemental and isotopic ratios, except for V/Al, exhibit a narrower range of values than literature data. This narrower range may reflect that our samples represent a smaller selection of rock types and formations compared to those studied previously from across the Andean volcanic zones. V/Al ratios on the other hand show a broader range of values, which may be due to the limited data published for V. Our work hence expands the V/Al endmember characterisation of Andean volcanics (Fig. 2). Lastly, although the overall ranges in Cd/Al, Ni/Al, Co/Al and 1/[Pb] ratios defined by the samples are smaller than found in previous studies, for each ratio our samples expand the overall data range. For example, the Ni/Al × 1000 ratios of our samples range from 0.005 to 0.4 whilst the literature range is from 0.02 to 3. Thus, an updated range for the Ni/Al × 1000 ratios of Andean volcanic deposits is 0.005–3 (Fig. 2).

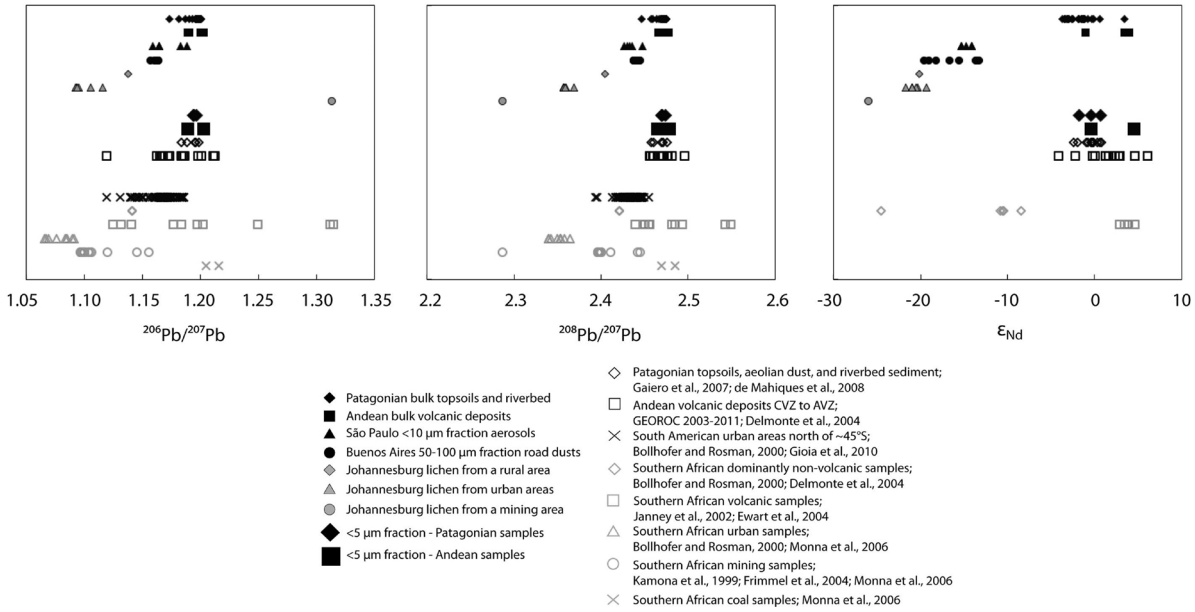

Fig. 3. Lead and Nd isotope compositions for samples from this study (filled symbols) and the literature (open symbols). All 2SD error bars are smaller than the size of the symbols.

3.1.3. Aerosols from São paulo

To our knowledge, there is no previously published multi-element dataset for aerosols from São Paulo. The Pb/Al, Zn/Al, Cu/Al, Cr/Al ratios are generally higher for these aerosols than for natural rocks and sediments from the São Paulo region (Fig. 2). For example Pb/Al × 1000 ranges from 50 to 100 and Zn/Al × 1000 span values from 300 to 900 for the aerosols (Fig. 2). In contrast, ore deposits exposed at São Paulo State, composed of lamprophyre, dioritic, carbonatitic and magnetitic rock types, exhibit Pb/Al × 1000 ratios of 1.5–60 and Zn/Al × 1000 ratios of 1–50 (Bertolo et al., 2011; Fig. 2). The $^{208}Pb/^{207}Pb$ ratios are low and in agreement with aerosols analysed between 1994 and 2005 from São Paulo (Bollhöfer and Rosman, 2000; Gioia et al., 2010; Fig. 3, Gioia et al., 2017). Lead, Zn, Cu and Cd are all chalcophile metals with similar geochemical behaviour and distribution, whilst Cr is a lithophile transition element generally associated with oxide phases. Enrichments in Pb, Zn, Cu, Cd and Cr and low Pb isotope ratios compared to natural sources are typical of industrial emissions, such as non-ferrous metal processing, smelting, waste incineration, and biomass, coal and oil combustion (e.g., Nriagu and Pacyna, 1988; Pacyna and Pacyna, 2001; Ulke and Andrade, 2001). Relatively low Pb isotope ratios have been found to correlate with some industrial and automobile emissions from São Paulo and other major cities in South America north of ~45°S (Bollhöfer and Rosman, 2000; Gioia et al., 2010; Gioia et al., 2017). This implies that Pb, Zn, Cu, Cd and Cr compositions exhibited by the aerosol samples from São Paulo are due to anthropogenic sources. The results also suggest that the main sources of anthropogenic aerosols in São Paulo have not changed significantly since 2005. As such, this study also provides improved constraints on the geochemical characteristics of anthropogenic aerosol sources in São Paulo.

Similarly, Nd isotope compositions have not been reported before for aerosols from São Paulo. We observe generally higher 1/[Nd] values for the aerosols compared to natural sources (Fig. 2) as well as low ε_{Nd} values of between −14.1 and −15.3 (Fig. 3). These results suggest that the aerosols derived from re-suspension of soils generated by the alteration of old Archean to Neoproterozoic rocks; supporting that the Nd values have been observed in re-worked particulates such as road dusts which can contain anthropogenic materials. It should be noted, however, that the low ε_{Nd} values reflect differences in regional geology and are not of direct anthropogenic origin.

3.1.4. Road dusts from Buenos Aires

The Pb/Al, Zn/Al, Cu/Al and Cd/Al ratios are fairly high in the selected size fractions of the road dust (50–75 µm and 75–100 µm), e.g., Pb/Al × 1000 ranges from 5 to 10 (Fig. 2). These elemental compositions overlap with previously reported data for < 50 to 100 µm grain size separates (Fujiwara et al., 2011; Fig. 2). This implies that there is no significant grain size effect on the Pb, Zn, Cu, and Cd concentrations of road dust from Buenos Aires, at least for grain sizes < 100 µm. The samples show distinctively higher Zn/Al, Cu/Al, and Cr/Al ratios than rocks from Buenos Aires (de Campos et al., 2012; Fig. 2). The high metal/Al ratios of the samples, compared to natural sources, support the interpretation that road dusts are generally a mixture of anthropogenic materials (i.e. traffic debris as well as vehicle and industrial emissions) in line with the study by Fujiwara et al. (2011).

To our knowledge Cr, V, Co, Sc, Y, Th, and REE data have not been previously reported for road dust from Buenos Aires. The high Cr/Al × 1000 ratios of 8–40 are most likely derived from anthropogenic sources, as they are accompanied by enrichments in other pollutant trace metals. Meanwhile, Co/Al, Ni/Al and V/Al ratios are comparable to geogenic rocks (Campos et al., 2012; Fig. 2), which suggest that not all metals in Buenos Aires road dust are affected by anthropogenic sources.

The Pb isotope analyses of the road dust samples yielded $^{208}Pb/^{207}Pb$ and $^{206}Pb/^{207}Pb$ ratios of between 2.4391 and 2.4448, and 1.1605–1.1626, respectively (Fig. 3), in line with aerosols from other major cities in South America and industrial and vehicle emissions from north of ~45° S (Bollhöfer and Rosman, 2000; Gioia et al., 2010, 2017; Fig. 3). Similarly, the Buenos Aires road dust displays ε_{Nd} values of between −13.3 and −19.6 (Fig. 3), which resembles ε_{Nd} values of aerosols from São Paulo. These similarities likely reflect that particulates in the road dust derived from rock with similar composition, of similar ages.

3.1.5. Lichen from a rural area from johannesburg

The lichen sample from a rural area near Johannesburg generally shows high trace element/Al ratios and high 1/[Pb] (with Pb/Al × 1000 = 2.5; Fig. 2) as well as unradiogenic Pb and very low ε_{Nd} values (e.g., $^{208}Pb/^{207}Pb$ = 2.4043; ε_{Nd} = −20.1; Fig. 3). This composition is within the range reported for non-volcanic rocks from around Johannesburg, central South Africa, and Namibia (Archean granitic

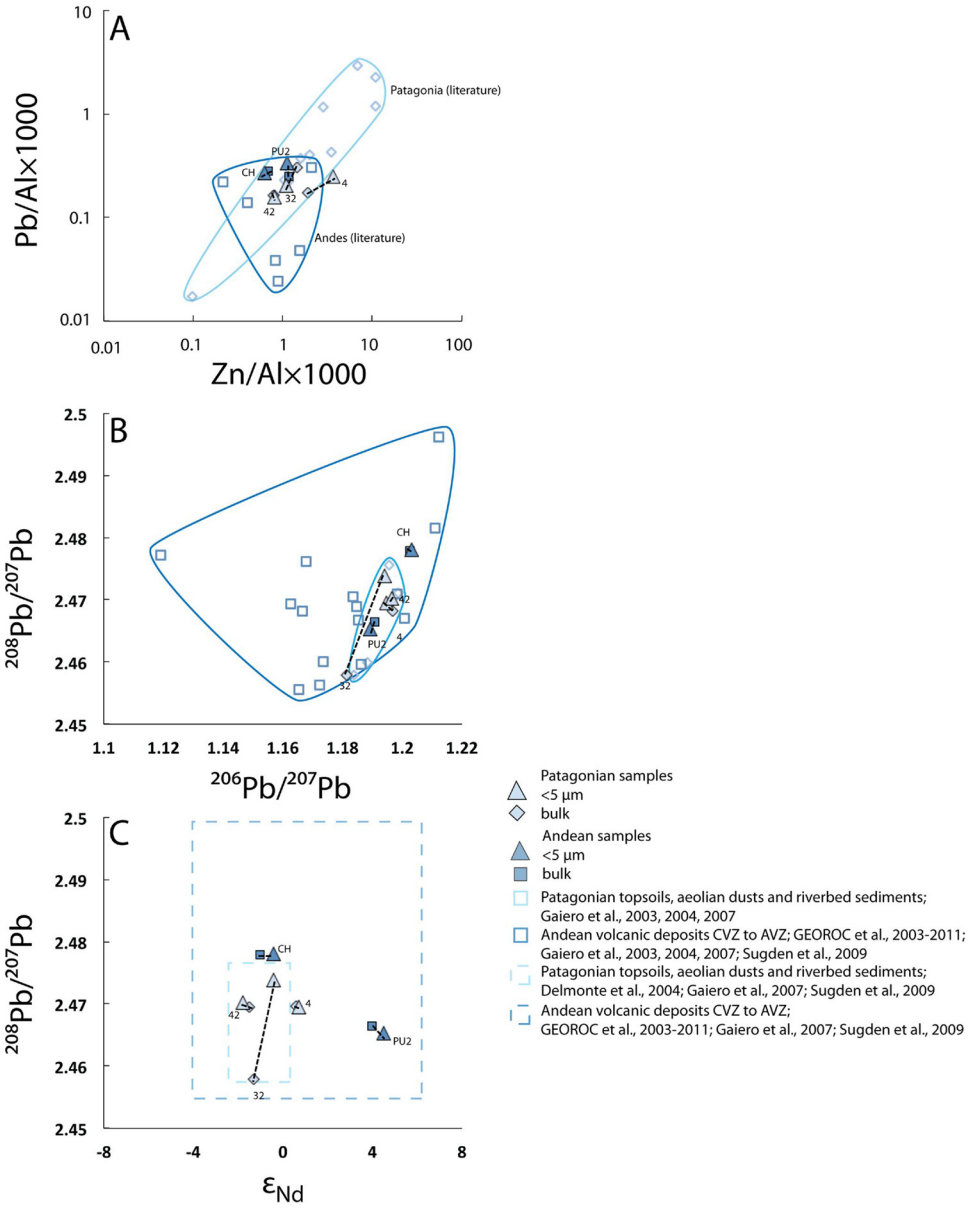

Fig. 4. (A) Pb/Al × 1000 vs. Zn/Al × 1000, (B) $^{208}Pb/^{207}Pb$ vs. $^{206}Pb/^{207}Pb$, and (C) $^{208}Pb/^{207}Pb$ vs. ε_{Nd} for the fine fractions (< 5 µm) and bulk powders of samples 4, 32, 42, CH, and PU2 from this study (filled symbols). Also shown are literature data for topsoils, riverbed sediments and dust from Patagonia, as well as volcanic rock and tephra from the Andean volcanic belt (open symbols). In Fig. 4C, the range of literature values for $^{208}Pb/^{207}Pb$ and ε_{Nd} is denoted by light blue and blue dashed boxes, respectively, as the Pb and Nd isotope results do not originate from the same studies. Dashed black lines connect the fine fractions and bulk powders of the same sample. All 1SD error bars are smaller than the size of the symbols. (For interpretation of the references to colour in this figure legend, the reader is referred to the web version of this article.)

rocks, ultramafic lavas, and metasedimentary rocks from the Barberton Region in South Africa; Condie and Hunter, 1976; lamprophyre and calk-alkaline formations, and lamprophyres and carbonatites from Damaraland in northern Namibia; Le Roex and Lanyon, 1998; aerosols from the Namib desert; Bollhöfer and Rosman, 2000; kimberlitic formations SW of Johannesburg from the Archean shield, Le Roex et al., 2003; Figs. 2 and 3).

Volcanic rocks from Southern Africa (e.g., mafic to ultramafic volcanics from the Etendeka Province in Namibia and along the Western Cape Province in South Africa; Janney et al., 2002; Ewart et al., 2004; Fig. 3) exhibit similar elemental compositions, but show more radiogenic Pb and Nd isotopic compositions than the rural lichen sample (Fig. 3). This suggests that the composition of the rural lichen predominantly records the Archean to Neoproterozoic geology (Tohver et al., 2006; Begg et al., 2009, Fig. 1). Little more can be inferred as only a single sample was analysed. To our knowledge, there are no reported Cd data for rural lichen samples from South Africa and our measurements suggest a Cd/Al × 1000 ratio of 0.03 (Fig. 2).

3.1.6. Lichen samples from an urban area of johannesburg

The lichen samples from urban areas of Johannesburg show high trace element/Al ratios (e.g., Pb/Al × 1000 and Zn/Al × 1000 range from 8 to 20; Fig. 2), except for V/Al and Co/Al. The $^{208}Pb/^{207}Pb$ and $^{206}Pb/^{207}Pb$ ratios are very low and vary from 2.3573 to 2.3692, and 1.0936–1.1162, respectively (Fig. 3). The trace element/Al ratios and 1/[Pb] are within the range of data for non-volcanic and volcanic regional rocks (Fig. 2). However, the Pb isotope ratios are lower than those of natural samples (Fig. 3), and are similar to previously published results for lichens from urban areas of Johannesburg (Monna et al., 2006) and aerosols from major cities across South Africa (Bollhöfer and Rosman, 2000) (Fig. 3). This demonstrates that Pb isotopic compositions reflect the Pb ores used in anthropogenic activities in South Africa, as acknowledged by Monna et al. (2006) and Bollhöfer and Rosman (2000), and suggests that they are useful indicators of anthropogenic sources. It is also evident that trace element/Al ratios are unable to clearly distinguish between anthropogenic and natural aerosol sources in Southern Africa, in contrast to the observations made for South America (Fig. 2).

3.1.7. Tree bark from a mining area from Johannesburg

To our knowledge, we here report the first multi-element data that characterises aerosol emissions from mining regions of Southern Africa

(Table S2-S3). Trace element/Al ratios are high for tree bark sample from a mine dump site in Johannesburg (e.g., Pb/Al × 1000 ≈ 8; Fig. 2). These ratios, as well as 1/[Pb] ratios, are either within the range or slightly elevated compared to regional source rocks (Fig. 2), whereby the trace element enrichments may be linked to emissions from the mine dump. For example, Pb/Al is higher than previously reported for non-volcanic rocks but in line with the upper range reported for volcanic rocks (Fig. 2). The Zn/Al ratio is in accord with previously reported data for non-volcanic rocks but higher than for regional volcanic rocks (Fig. 2). The $^{208}Pb/^{207}Pb$ ratio for the tree bark from the mine dump site is very low at 2.2866, while the $^{206}Pb/^{207}Pb$ ratio is relatively high at 1.3133 (Fig. 3). Notably, $^{208}Pb/^{207}Pb$ agrees well with previously reported values for South African mining samples (Monna et al., 2006), but the $^{206}Pb/^{207}Pb$ ratio is higher than data previously reported for a number of other regions (i.e. ore deposits from carbonate-hosted sulphide deposits in Kabwe, Tsumeb and Kipushi, Namibia; Kamona et al., 1999; ore deposits from Rosh Pinah Mine, Namibia; Frimmel et al., 2004). The differences in Pb isotopic compositions between mining areas are most likely due to variations in the ages and U-Th/Pb ratios of ores. For example, the high $^{206}Pb/^{207}Pb$ ratio of the tree bark sample analysed here may reflect the high uranium levels associated with the Witwatersrand goldfields 5 km west of Johannesburg (Monna et al., 2006).

The lichen from rural and urban areas, and tree bark from the mining area present ε_{Nd} values between about −19 and −26, which are generally lower than results reported for regional rocks (Fig. 3). This is most likely because the Nd derived from relatively older rock formations as observed in South America.

3.2. Particle size effect on elemental and isotopic composition

Two topsoil samples, one riverbed sediment from Patagonia, and two volcanic tephra samples from the Chaiten and Puyehue volcanoes were chosen to explore whether element ratios and isotopic compositions show a difference between the fine (< 5 μm) fractions and bulk powders of source samples. Results for Pb/Al and Zn/Al ratios, and Nd and Pb isotopic compositions are shown in Fig. 4.

Overall, differences that exceed the analytical uncertainties can be observed for both, elemental concentrations and isotopic compositions. For example, the Pb/Al × 1000 ratios of fine fractions and bulk samples differ by ~0.05 to 0.10 for samples 4, 32 and PU2 (Fig. 4A). The observed differences are, however, not unidirectional and are element specific. Sample 32 exhibits the greatest difference in Pb/Al × 1000, whilst sample 4 shows the biggest difference in the Zn/Al × 1000 ratio (Fig. 4A). Differences in Pb isotope compositions between fine fractions and bulk samples range between 0.0003 and 0.0160, exceeding the analytical uncertainty (Fig. 4B). The observed differences in element ratios and Pb isotopic compositions between fine fractions and bulk powders are expected, as different minerals can show distinct elemental compositions, including variable U/Pb and Th/Pb ratios (e.g., Feng et al., 2010). This in turn results in particle size control on sample compositions and/or elemental/isotopic heterogeneity in individual samples. The ε_{Nd} values of fine fractions and bulk samples show differences of between 0.3 and 0.9, which are notable but not clearly resolvable, given the analytical uncertainty (Fig. 4C). In line with recent literature, particle size hence does not significantly affect the ε_{Nd} values of rural and volcanic aerosol source regions in South America (e.g., Feng et al., 2009; Meyer et al., 2011).

The Pb/Al, Zn/Al, $^{208}Pb/^{207}Pb$ ratios and ε_{Nd} values of the fine fractions and bulk samples fall within the range of previously reported data for fine fractions and bulk powder samples from similar rural areas (fine and < 63 μm fractions of topsoils, riverbed sediment and dust; Fig. 4) and volcanic sources (fine fractions and bulk volcanic rock and tephra; Fig. 4) from South America (e.g., 1.1191–1.2124 in $^{206}Pb/^{207}Pb$ and 2.4555–2.4964 in $^{208}Pb/^{207}Pb$ for volcanic sources from South America, Fig. 4B; ε_{Nd} values of −8.9 to +8.3 and of −4.2 to +6.1 for rural and volcanic sources from South America, Fig. 4C). Given the observed variations in elemental and isotopic compositions between the fine fractions and bulk samples from Patagonia and the Andes, it is important to note that these differences are significantly smaller than the variability of elemental and isotopic compositions for various sampling sites across South America. In particular, the variability associated with particle size is smaller than compositional differences between samples of anthropogenic versus natural origin, for example between samples from Patagonia and the Andes versus samples from São Paulo and Buenos Aires (Fig. 2). This suggests that the effect of particle size on composition does not significantly affect the ability of key geochemical parameters to discriminate between different aerosol sources.

3.3. Summary of regions delineated by new and published geochemical data from South America and Southern Africa

Our new data provide important insights into source characteristics of key aerosol source regions of South America and South Africa. For example, the data for Patagonia and the Andes provide novel insights into the Cd concentrations of these natural sources and we also present the first set of combined multi-element and isotopic data for anthropogenic aerosols from São Paulo, to supplement the existing database of anthropogenic sources from South America. A further example is the Pb isotope signal of urban sources from Southern Africa, collected before the ban of leaded fuel. The current Pb isotope signal for urban sources from Southern Africa may trend towards a more natural source signal than we report in this study. However, the limited number of samples, as well as the geographical bias inherent to a small sample set, prevents application of the new results as a stand-alone dataset for characterising the aerosol sources of the South Atlantic Ocean. In conjunction with literature data, however, the geochemical characterisation of South American and South African sources can be revisited and suitable tracers for key source areas and types of materials can be identified.

The NVZ is beyond the range of typical westerly wind circulation across South America, which carries aerosols to the South Atlantic. However, seasonal and unusual weather patterns may be associated with transports of volcanic particulates from the NVZ to the South Atlantic. We hence consider the geochemical characterisation of volcanic deposits from the NVZ an important addition to existing data sets. Patagonia and the Andes can be classified as a single major source region for natural aerosols in South America, as it is difficult to distinguish the two areas based on elemental or isotopic compositions (Fig. 2). This reflects the occurrence and dispersal of similar volcanic deposits and rocks with Phanerozoic and younger age across Patagonia and the Andes (Almeida et al., 2000).

Urban regions situated north of ~45°S in South America can be collectively termed as the most significant anthropogenic aerosol source of South America, whereby the anthropogenic signal is primarily derived from industrial and vehicle emissions (Bollhöfer and Rosman, 2000; Fujiwara et al., 2011). The elements Pb, Zn, Cu and Cd are hence most likely to show elevated concentrations due to the anthropogenic activities in these urban areas.

For Southern Africa, the natural aerosol sources fall into two groups that feature distinct elemental and isotopic signatures. One of these is dominated by the old continental crust of the Archean shield, which is primarily non-volcanic. In contrast, the other group is mainly represented by volcanic deposits of younger Phanerozoic age. The anthropogenic aerosol sources of Southern Africa can be sub-divided into urban as well as mining- and coal-related sources. Industrial and vehicle emissions as well as mining and coal combustion are important anthropogenic activities in Southern Africa and that some geochemical data is available for such sources from previous work (e.g., Bollhöfer and Rosman, 2000; Monna et al., 2006).

Table 2
Proposed characteristic elemental and isotopic composition of potential aerosol sources from South America and Southern Africa.

Continent	Category	Sub-category	Pb/Al x1000	Zn/Al x1000	Cu/Al x1000	Cd/Al x1000	V/Al x1000	Ni/Al x1000	Cr/Al x1000
South America									
	Natural		0.02 − 3	0.1 − 10	0.04 − 3	0.0006 − 0.008	0.06 − 3	0.005 − 4	0.1 − 10
	Anthropogenic	urban	4 − 100	8 − 900	2 − 60	0.01 − 5	0.9 − 20	0.3 − 20	8 − 900
South Africa									
	Natural	non-volcanic	0.06 − 3	0.5 − 20	0.07 − 10	0.03	0.4 − 10	0.1 − 400	0.5 − 20
		volcanic	0.03 − 6	1 − 2	2 − 3	0.001 − 0.006	3 − 5	0.6 − 3	1 − 2
	Anthropogenic	urban	8 − 20	10 − 20	3 − 6	0.02 − 0.05	2 − 3	1 −2	10 − 20
		mine	8	30	7	0.1	3	6	30
		coal							

Continent	Category	Sub-category	Co/Al x1000	1/[Pb] 1/[μg/g]	1/[Nd] 1/[μg/g]	$^{208}Pb/^{207}Pb$	$^{206}Pb/^{207}Pb$	ε_{Nd}
South America								
	Natural		0.02 − 20	0.0004 − 0.4	0.02 − 0.2	2.4465 − 2.4962	1.1191 − 1.2111	-4.2 to +6.1
	Anthropogenic	urban	0.1 − 3	0.0002 − 0.01	0.02 − 0.8	2.3950 − 2.4548	1.1190 − 1.1887	-19.6 to −13.3
South Africa								
	Natural	non-volcanic	0.05 − 30	0.02 − 2	0.003 − 0.3	2.4043 − 2.4210	1.1380 − 1.1410	-24.5 to −8.4
		volcanic	0.05 − 0.07	0.002 − 0.4	0.01 −0.06	2.4390 − 2.5493	1.1245 − 1.3149	+2.9 to +4.6
	Anthropogenic	urban	0.3 − 0.4	0.003 − 0.02	0.2 − 0.4	2.3420 − 2.4472	1.0690 − 1.1162	-21.7 to −19.4
		mine	5	0.004 − 0.1	0.6	2.3994 − 2.4420	1.0965 − 1.1556	−26.0
						2.2865 − 2.2866	1.3133	
		coal		0.06 − 0.1		2.4691 − 2.4853[a]	1.2050 − 1.2190[a]	

[a] Data taken from – Monna et al., 2006.

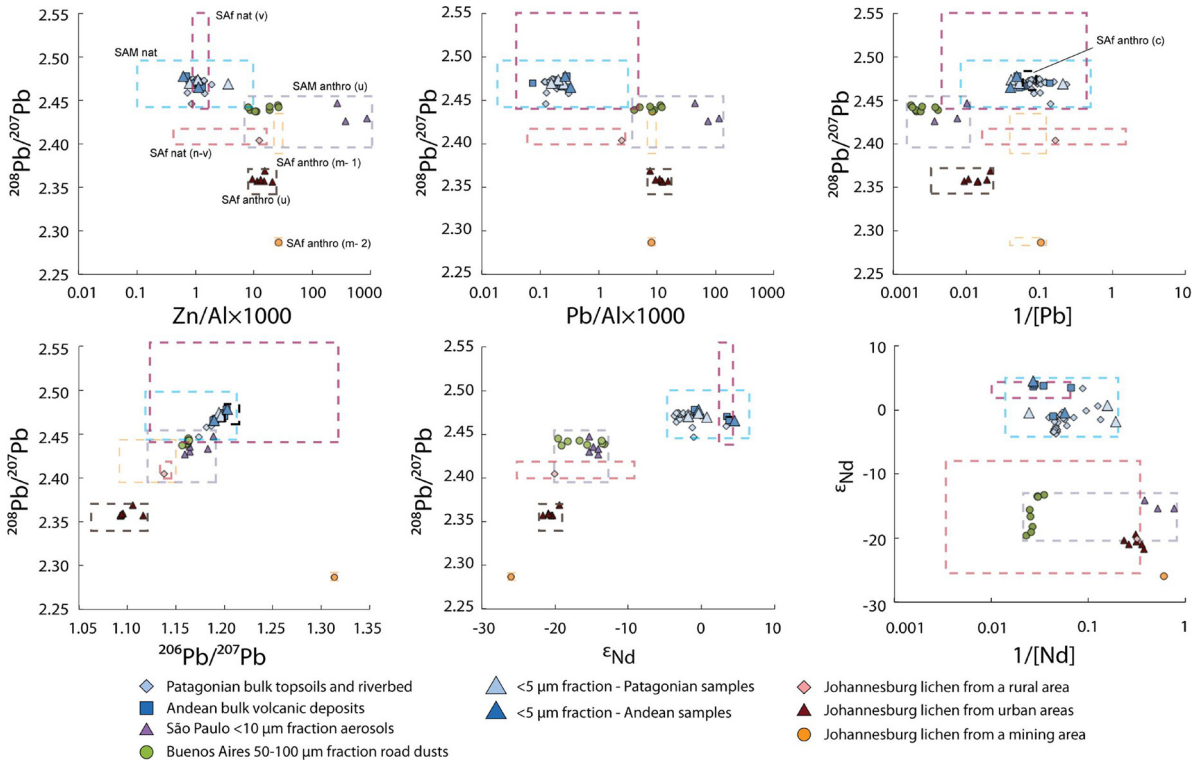

Fig. 5. Bivariate plots of elemental and isotopic compositions for the suggested natural (nat) and anthropogenic (anthro) aerosol sources of South America (SAM) and Southern Africa (SAf). Other abbreviations: v = volcanic, *n*-v = non-volcanic, u = urban, m-1 = mining group 1, m-2 = mining group 2, and c = coal sources. The symbols denote data from this study, whilst the stippled boxes outline the geochemical signature of a source, which was determined from our new data and literature results. All 2SD error bars are smaller than the size of the symbols.

3.4. Recommendations on geochemical proxies to distinguish aerosol sources from South America and Southern Africa

The elemental and isotopic data for natural and anthropogenic aerosol sources that were acquired in this study (Table 2) and compiled from the literature is of utility to studies that aim to constrain the origin of marine aerosols, particularly from the South Atlantic Ocean. Fig. 5 shows the geochemical parameters that are best suited to distinguish (i) natural from anthropogenic aerosol sources, and (ii) South American from Southern African sources.

In South America, anthropogenic aerosol sources are characterised by relatively high Pb/Al, Cd/Al, Zn/Al, and Cu/Al ratios as well as lower Pb isotope ratios compared to the major natural sources (Fig. 5), and have shown association with low ε_{Nd} values. Important natural and anthropogenic aerosol sources of South America are well separated in bi-variant plots of $^{208}Pb/^{207}Pb$ vs. ε_{Nd}, $^{208}Pb/^{207}Pb$ vs. Pb/Al, 1/[Pb], Zn/Al, Cd/Al, Cu/Al, and plots of ε_{Nd} vs. Pb/Al, and 1/[Nd] (Fig. 5). Pb/Al, Zn/Al, Cu/Al and Cd/Al ratios of aerosols in São Paulo are distinctly higher than in Buenos Aires aerosols. Whilst this may be related to the distinct origins of the aerosols from the two cities, it may also reflect the higher levels of anthropogenic activity in São Paulo, as a consequence of the much larger area and population of São Paulo (approx. 1500 km^2 with 11 million inhabitants) in comparison to Buenos Aires (approx. 200 km^2 with 3 million inhabitants). Furthermore, the higher 1/[Nd] values of São Paulo versus Buenos Aires aerosols separate the two urban source regions, whereby the aerosol Nd concentrations may reflect the distinct characteristics (e.g., mineralogy) of the respective source emissions and/or areas (e.g., Gallet et al., 1996; Chang et al., 2000; Zdanowicz et al., 2006; Ferrat et al., 2011).

In Southern Africa, the non-volcanic aerosol sources display lower Pb isotope ratios (e.g., $^{208}Pb/^{207}Pb$) and ε_{Nd} values than the volcanic sources (Fig. 5). Literature data for coal samples from Johannesburg were included in Fig. 4 to constrain the likely geochemical variation between coal-related and other sources from Southern Africa. However, the sample numbers are limited (n = 2) and the only geochemical data available are Pb concentration and isotopic compositions (Monna et al., 2006). Fig. 4 suggests that South African natural sources have lower Pb/Al and higher Pb isotope ratios than urban and mining-related sources of Southern Africa. Non-volcanic and volcanic rocks display higher 1/[Pb] than lichen and other urban samples in Southern Africa (Fig. 5), which confirms that higher Pb concentrations are generally associated with the emission of anthropogenic Pb in urban areas. The volcanic and coal-related aerosol sources of Southern Africa show similar Pb isotope ratios, which are generally higher than the Pb isotope ratios of urban and mining-related source areas (Fig. 5). This difference presumably reflects that anthropogenic Pb is primarily associated with older ore deposits that record a long-term evolution with low U/Pb and Th/Pb ratios. Similarly, volcanic rocks can be discriminated from lichen and ores by higher ε_{Nd} values (Fig. 5), but keeping in mind that these variations in ε_{Nd} are of geological and not of anthropogenic origin.

The urban sources of South America are separated from the Southern African urban sources by the higher $^{206}Pb/^{207}Pb$ and $^{208}Pb/^{207}Pb$ ratios of the former (Fig. 5). This suggests that anthropogenic sources of Pb in South America are derived from younger ore bodies than in Southern Africa. Southern African non-volcanic, urban, and mine-related, and South American urban aerosol sources can be distinguished from the volcanic sources of Southern Africa and non-volcanic and volcanic sources of South America by the less radiogenic ε_{Nd} values of the former (Fig. 5). Finally, plots of $^{208}Pb/^{207}Pb$ vs. 1/[Pb] separate the Southern African rural, volcanic as well as mine- and coal-related sources from the South American urban sources (Fig. 5).

4. Conclusions

This study significantly expands the elemental (major, trace and rare earth elements) and isotopic (Pb and Nd isotope) data that is

available to characterise and discriminate between important South American and South African aerosol sources to the South Atlantic Ocean. This was achieved by analysing a wide range of natural and anthropogenic samples, including road dust from Buenos Aires, aerosols from São Paulo, soil dust from Patagonia, and volcanic deposits from the Andean volcanic belt as well as various lichen from urban and rural areas of South Africa. A geochemical comparison of the fine fraction (< 5 μm) and bulk powder samples of selected mineral dust samples from Patagonia and the Andes suggest a significant impact of particle size on composition. The effect is however small when compared to observed geochemical variations between the different aerosol sources of South America and Southern Africa.

Based on a detailed evaluation of our new aerosol source data and comprehensive compilation of relevant data from the literature, we propose a set of geochemical parameters that is able to distinguish between natural and anthropogenic aerosols that reach the South Atlantic Ocean from both, South America and Southern Africa. These encompass discrimination plots of $^{208}Pb/^{207}Pb$ vs. ε_{Nd}, $^{208}Pb/^{207}Pb$ vs. Pb/Al, 1/[Pb], Zn/Al, Cd/Al, Cu/Al, and diagrams of ε_{Nd} vs. Pb/Al and 1/[Nd]. As such, our study has developed new and powerful tools for future studies that aim to trace and quantify the trace metal and nutrient inputs from aerosols to the South Atlantic Ocean.

Acknowledgements

This study was supported by the NERC grant NE/H005390/1. We would like to acknowledge the CLIM-Amazon project for their financial support of RK (GA no. 295091–project Inco-LAB FP7 supported by the EC).

Appendix A. Supplementary data

Supplementary data associated with this article can be found, in the online version, at https://doi.org/10.1016/j.chemer.2018.05.001.

References

Alkmim, F.F., Marshak, S., Fonseca, M.A., 2001. Assembling west gondwana in the neoproterozoic: clues from the São francisco craton region, Brazil. Geology 29 (4), 319–322. http://dx.doi.org/10.1130/0091-7613(2001)029<0319:awgitn>2.0.co;2.

Almeida, F.F.M., Neves, B.B.D., Carneiro, C.D., 2000. The origin and evolution of the South American Platform. Earth Sci. Rev. 50 (1–2), 77–111.

Babinski, M., Aily, C., Ruiz, I.R., Sato, K., 2003. Pb isotopic signatures of the atmosphere of the São Paulo city, Brazil. J. De Physique IV 107 (1), 87–90.

Begg, G.C., Griffin, W.L., Natapov, L.M., O'Reilly, S.Y., Grand, S.P., O'Neill, C.J., Bowden, P., 2009. The lithospheric architecture of Africa: seismic tomography, mantle petrology, and tectonic evolution. Geosphere 5 (1), 23–50. http://dx.doi.org/10.1130/ges00179.1.

Bertolo, R., Bourotte, C., Marcolan, L., Oliveira, S., Hirata, R., 2011. Anomalous content of chromium in a Cretaceous sandstone aquifer of the Bauru Basin, state of São Paulo Brazil. J. South Amer. Earth Sci. 31, 69–80.

Bollhöfer, A., Rosman, K.J.R., 2000. Isotopic source signatures for atmospheric lead: the Southern Hemisphere. Geochim. Cosmochim. Acta 64 (19), 3251–3262. http://dx.doi.org/10.1016/s0016-7037(00)00436-1.

Boyd, P.W., Watson, A.J., Law, C.S., Abraham, E.R., Trull, T., Murdoch, R., Zeldis, J., 2000. A mesoscale phytoplankton bloom in the polar Southern Ocean stimulated by iron fertilisation. Nature 407 (6805), 695–702. http://dx.doi.org/10.1038/35037500.

Brito Neves, B.B., Fuck, R.A., 2013. Neoproterozoic evolution of the basement of the South-American platform. J. South Am. Earth Sci. 47, 72–89. http://dx.doi.org/10.1016/j.jsames.2013.04.005.

Campos, R.S., Philipp, R.P., Massonne, H.-J., Chemale Jr, F., 2012. Early post-collisional Brasiliano magmatism in Botuverá region, Santa Catarina, Southern Brazil: evidence from petrology, geochemistry, isotope geology and geochronology of the diabase and lamprophyre dikes. J. South Am. Earth Sci. 37, 266–278.

Chang, Q., Mishima, T., Yabuki, S., Takahashi, Y., Shimizu, H., 2000. Sr and Nd isotope ratios and REE abundances of moraines in the mountain areas surrounding the Taklimakan Desert, NW China. Geochem. J. 34 (6), 407–427.

Chin, M., 2009. Dust Emission, Transport and Effects on Air Quality: A Global Model Simulation and Comparison with Multi-platform Data. NASA Goddard Space Flight.

Condie, K., Hunter, D., 1976. Trace element geochemistry of Archean granitic rocks from the Barberton region, South Africa. Earth Planet. Sci. Lett. 29 (2), 389–400.

Delmonte, B., Basile-Doelsch, I., Petit, J.R., Maggi, V., Revel-Rolland, M., Michard, A., Grousset, F., 2004. Comparing the Epica and Vostok dust records during the last 220,000 years: stratigraphical correlation and provenance in glacial periods. Earth Sci. Rev. 66 (1–2), 63–87. http://dx.doi.org/10.1016/j.earscirev.2003.10.004.

Desboeufs, K.V., Losno, R., Colin, J.L., 2001. Factors influencing aerosol solubility during cloud processes. Atmos. Environ. 35 (20), 3529–3537. http://dx.doi.org/10.1016/s1352-2310(00)00472-6.

Dostal, J., Zentilli, M., Caelles, J.C., Clark, A.h., 1977. Geochemistry and origin of volcanic rocks of the Andes (26–28S). Contrib. Miner. Petrol. 63, 113–128.

Ducart, D.F., Crosta, A.P., Souza Filho, C.R., Coniclio, J., 2006. Alteration mineralogy at the Cerro La Mina epithermal prospect, Patagonia Argentina: field mapping, shortwave infrared spectroscopy, and ASTER images. Econ. Geol. 101 (5), 981–996. http://dx.doi.org/10.2113/gsecongeo.101.5.981.

Ebert, P., Baechmann, K., 1998. Solubility of lead in precipitation as a function of raindrop size. Atmos. Environ. 32 (4), 767–771. http://dx.doi.org/10.1016/s1352-2310(97)00344-0.

Ewart, A., Marsh, J.S., Milner, S.C., Duncan, A.R., Kamber, B.S., Armstrong, R.A., 2004. Petrology and geochemistry of early cretaceous bimodal continental flood volcanism of the NW Etendeka, Namibia. Part 1: Introduction, mafic lavas and re-evaluation of mantle source components. J. Petrol. 45 (1), 59–105. http://dx.doi.org/10.1093/petrology/egg083.

Feng, J.-L., Zhu, L.-P., Zhen, X.-L., Hu, Z.-G., 2009. Grain size effect on Sr and Nd isotopic compositions in eolian dust: implications for tracing dust provenance and Nd model age. Geochem. J. 43, 123–131.

Feng, J.-L., Hu, Z.G., Cui, J.Y., Zhu, L.P., 2010. Distributions of lead isotopes with grain size in aeolian deposits. Terra Nova 22 (4), 257–263. http://dx.doi.org/10.1111/j.1365-3121.2010.00941.x.

Ferrat, M., Weiss, D.J., Strekopytov, S., Dong, S., Chen, H., Najorka, J., Sinha, R., 2011. Improved provenance tracing of Asian dust sources using rare earth elements and selected trace elements for palaeomonsoon studies on the eastern Tibetan Plateau. Geochim. Cosmochim. Acta 75 (21), 6374–6399. http://dx.doi.org/10.1016/j.gca.2011.08.025.

Frimmel, H.E., Jonasson, I.R., Mubita, P., 2004. An Eburnean base metal source for sediment-hosted zinc-lead deposits in Neoproterozoic units of Namibia: lead isotopic and geochemical evidence. Miner. Deposita 39 (3), 328–343. http://dx.doi.org/10.1007/s00126-004-0410-7.

Fujiwara, F., Rebagliati, R.J., Dawidowski, L., Gómez, D., Polla, G., Pereyra, V., Smichowski, P., 2011. Spatial and chemical patterns of size fractionated road dust collected in a megacitiy. Atmos. Environ. 45 (8), 1497–1505. http://dx.doi.org/10.1016/j.atmosenv.2010.12.053.

GEOROC (2003–2011). Geochemistry of Rocks of the Oceans and Continents. Website (http://www.georoc.mpch-mainz.gwdg.de/georoc/).

Gaiero, D.M., Probst, J.L., Depetris, P.J., Bidart, S.M., Leleyter, L., 2003. Iron and other transition metals in Patagonian riverborne and windborne materials: geochemical control and transport to the southern South Atlantic Ocean. Geochim. Cosmochim. Acta 67 (19), 3603–3623. http://dx.doi.org/10.1016/s0016-7037(03)00211-4.

Gaiero, D.M., Depetris, P.J., Probst, J.-L., Bidart, S.M., Leleyter, L., 2004. The Signature of River- and Wind-Borne Material Exported from Patagonia to the Southern Latitudes: A View from REEs and Implications for Paleoclimatic Interpretations. GCA.

Gaiero, D.M., Brunet, F., Probst, J.-L., Depetris, P.J., 2007. A uniform isotopic and chemical signature of dust exported from Patagonia: rock sources and occurrence in southern environments. Chem. Geol. 238 (1–2), 107–120. http://dx.doi.org/10.1016/j.chemgeo.2006.11.003.

Gallet, S., Jahn, B.M., Torii, M., 1996. Geochemical characterisation of the Luochuan loess-paleosol sequence, China: and paleoclimatic implications. Chem. Geol. 133, 67–88.

Galloway, J.N., Dentener, F.J., Capone, D.G., Boyer, E.W., Howarth, R.W., Seitzinger, S.P., Vorosmarty, C.J., 2004. Nitrogen cycles: past, present, and future. Biogeochemistry 70 (2), 153–226. http://dx.doi.org/10.1007/s10533-004-0370-0.

Gasso, S., Stein, A.F., 2007. Does dust from Patagonia reach the sub-Antarctic Atlantic ocean? Geophys. Res. Lett. 34 (1). http://dx.doi.org/10.1029/2006gl027693.

Gioia, S.M.C.L., Babinski, M., Weiss, D.J., Kerr, A.A.F.S., 2010. Insights into the dynamics and sources of atmospheric lead and particulate matter in São Paulo Brazil, from high temporal resolution sampling. Atmos. Res. 98 (2–4), 478–485. http://dx.doi.org/10.1016/j.atmosres.2010.08.016.

Gioia, S.M.C.L., Babinski, M., Weiss, D.J., Spiro, B., Kerr, A., Veríssimo, T.G., Ruiz, I.R., Prates, J.C.M., 2017. An isotopic study of atmospheric lead in a megacity after phasing out of leaded gasoline. Atmos. Environ. 149, 70–83.

Grunder, A.L., 1987. Low delta-O-18 silicic volcanic-rocks at the calabozos caldera complex, Southern Andes − Evidence for Upper-Crustal contamination. Contrib. Miner. Petrol. 95 (1), 71–81. http://dx.doi.org/10.1007/bf00518031.

Honda, M., Yabuki, S., Shimizu, H., 2004. Geochemical and isotopic studies of aeolian sediments in China. Sedimentology 51 (2), 211–230. http://dx.doi.org/10.1046/j.1365-3091.2003.00618.x.

Hsu, S.-C., Wong, G.T.F., Gong, G.-C., Shiah, F.-K., Huang, Y.-T., Kao, S.-J., Tseng, C.-M., 2010. Sources, solubility, and dry deposition of aerosol trace elements over the East China Sea. Mar. Chem. 120 (1–4), 116–127. http://dx.doi.org/10.1016/j.marchem.2008.10.003.

Jacobsen, S.B., Wasserburg, G.J., 1980. Sm-Nd isotopic evolution of chondrites. Earth Planet. Sci. Lett. 50 (1), 139–155. http://dx.doi.org/10.1016/0012-821x(80)90125-9.

Jakes, P., White, A.J.R., 1972. Hornblendes from calc-alkaline volcanic-rocks of island arcs and continental margins. Am. Mineral. 57 (5–6), 887.

Janney, P.E., Le Roex, A.P., Carlson, R.W., Viljoen, K.S., 2002. A chemical and multi-isotope study of the Western Cape olivine melilitite province, South Africa: implications for the sources of kimberlites and the origin of the HIMU signature in Africa. J. Petrol. 43 (12), 2339–2370. http://dx.doi.org/10.1093/petrology/43.12.2339.

Johnson, M.S., Meskhidze, N., Solmon, F., Gasso, S., Chuang, P.Y., Gaiero, D.M., Yantosca, R.M., Wu, S., Wang, Y., Carouge, C., 2010. Modeling dust and soluble iron deposition to the South Atlantic Ocean. J. Geophys. Res. 115, D15202. http://dx.doi.org/10.1029/12009JD013311.

Kamona, A.F., Leveque, J., Friedrich, G., Haack, U., 1999. Lead isotopes of the carbonate-hosted Kabwe Tsumeb, and Kipushi Pb-Zn-Cu sulphide deposits in relation to Pan African orogenesis in the Damaran-Lufilian Fold Belt of Central Africa. Miner. Deposita 34 (3), 273–283. http://dx.doi.org/10.1007/s001260050203.

Kay, S.M., Ardolino, A.A., Gorring, M.L., Ramos, V.A., 2006. The somuncura large igneous province in patagonia: interaction of a transient mantle thermal anomaly with a subducting slab. J. Petrol. 48 (1), 43–77. http://dx.doi.org/10.1093/petrology/egl053.

Le Roex, A.P., Lanyon, R., 1998. Isotope and trace element geochemistry of Cretaceous Damaraland lamprophyres and carbonatites, northwestern Namibia: evidence for plume-lithosphere interactions. J. Petrol. 39 (6), 1117–1146.

Le Roex, A.P., Bell, D.R., Davis, P., 2003. Petrogenesis of group I kimberlites from Kimberley, South Africa: evidence from bulk-rock geochemistry. J. Petrol. 44 (12), 2261–2286. http://dx.doi.org/10.1093/petrology/egg077.

Li, F., Ginoux, P., Ramaswamy, V., 2008. Distribution, transport, and deposition of mineral dust in the Southern Ocean and Antarctica: contribution of major sources. J. Geophys. Res-Atmos. 113 (D10), D10. http://dx.doi.org/10.1029/2007jd009190.

Mahiques, M.M., Tassinari, C.C.G., Marcolini, S., Violante, R.A., Figueira, R.C.L., Silveira, I.C.A., Burone, L., Mello e Sousa, S.H., 2008. Nd and Pb isotope signatures on the Southeastern South American upper margin: implications for sediment transport and source rocks. Mar. Geol. 250, 51–63.

Mahowald, N.M., Baker, A.R., Bergametti, G., Brooks, N., Duce, R.A., Jickells, T.D., Tegen, I., 2005. Atmospheric global dust cycle and iron inputs to the ocean. Global Biogeochem. Cycles 19 (4). http://dx.doi.org/10.1029/2004gb002402.

Mahowald, N.M., Engelstaedter, S., Luo, C., Sealy, A., Artaxo, P., Benitez-Nelson, C., Bonnet, S., Chen, Y., Chuang, P.Y., Cohen, D.D., Dulac, F., Herut, B., Johansen, A.M., Kubilay, N., Losno, R., Maenhaut, W., Paytan, A., Prospero, J.M., Shank, L.M., Siefert, R.L., 2009. Atmospheric iron deposition: global distribution, variability: and human perturbations. Ann. Rev. Ma. Sci. 1, 245–278.

Marfil, S., Maiza, P., 2012. Geochemistry of Hydrothermal Alteration in Volcanic Rocks. INTECH Open Access Publisher.

Meskhidze, N., Nenes, A., Chameides, W.L., Luo, C., Mahowald, N., 2007. Atlantic Southern Ocean productivity: fertilisation from above or below? Global Biogeochem. Cycles 21 (2). http://dx.doi.org/10.1029/2006gb002711. (n/a-n/a).

Meyer, I., Davies, G.R., Stuut, J.-B.W., 2011. Grain size control on Sr-Nd isotope provenance studies and impact on paleoclimate reconstructions: an example from deep-sea sediments offshore NW Africa. Geochem. Geophys. Geosyst. 12, 3.

Monna, F., Poujol, M., Losno, R., Dominik, J., Annegarn, H., Coetzee, H., 2006. Origin of atmospheric lead in Johannesburg, South Africa. Atmos. Environ. 40 (34), 6554–6566. http://dx.doi.org/10.1016/j.atmosenv.2006.05.064.

Morel, F.M.M., Milligan, A.J., Saito, M.A., 2003. Marine bioinorganic chemistry: the role of trace metals in the oceanic cycles of major nutrients. In: Elderfield, H. (Ed.), In The Oceans and Marine Geochemistry. Treatise on Geochemistry. Elsevier, Oxford.

Nriagu, J.O., Pacyna, J.M., 1988. Quantitative assessment of worldwide contamination of air, water, and soils by trace-metals. Nature 333 (6169), 134–139. http://dx.doi.org/10.1038/333134a0.

Pacyna, J.M., Pacyna, E.G., 2001. An assessment of global and regional emissions of trace metals to the atmosphere from anthropogenic sources worldwide. Environ. Rev. 9, 269–298.

Piketh, S.J., 2002. Chemical evidence of long-range atmospheric transport over southern Africa. J. Geophys. Res. 107 (D24). http://dx.doi.org/10.1029/2002jd002056.

Pin, C., Zalduegui, J.F.S., 1997. Sequential separation of light rare-earth elements, thorium and uranium by miniaturized extraction chromatography: application to isotopic analyses of silicate rocks. Anal. Chim. Acta 339 (1–2), 79–89. http://dx.doi.org/10.1016/s0003-2670(96)00499-0.

Prokop, Z., Curp, P., Zlevorova-Zlamalikova, V., Komarek, J., Dusek, L., Holoubek, I., 2003. Mobility, bioavailability, and toxic effects of cadmium in soil samples. Environ. Res. 91 (2), 119–126.

Prospero, J.M., Ginoux, P., Torres, O., Nicholson, S.E., Gill, T.E., 2002. Environmental characterisation of global sources of atmospheric soil dust identified with the Nimbus 7 Total Ozone Mapping Spectrometer (TOMS) absorbing aerosol product. Rev. Geophys. 40 (1). http://dx.doi.org/10.1029/2000rg000095.

Raes, F., Van Dingenen, R., Vignati, E., Wilson, J., Putaud, J.P., Seinfeld, J.H., Adams, P., 2000. Formation and cycling of aerosols in the global troposphere. Atmos. Environ. 34 (25), 4215–4240. http://dx.doi.org/10.1016/s1352-2310(00)00239-9.

Rapela, C.W., Kay, S.M., 1988. Late Paleozoic to recent magmatic evolution of Northern Patagonia. Episodes 11 (3), 175–182.

Rosello, E., Haring, C., Cardinali, G., Suarez, F., Laffitte, G., Nevistic, A., 2008. Hydrocarbons and petroleum geology of Tierra del Fuego, Argentina. Geologica Acta 6 (1), 69–83.

Sholkovitz, E.R., Sedwick, P.N., Church, T.M., 2009. Influence of anthropogenic combustion emissions on the deposition of soluble aerosol iron to the ocean: empirical estimates for island sites in the North Atlantic. Geochim. Cosmochim. Acta 73 (14), 3981–4003. http://dx.doi.org/10.1016/j.gca.2009.04.029.

Spokes, L.J., Jickells, T.D., Lim, B., 1994. Solubilisation of aerosol trace-metals by cloud processing –A laboratory study. Geochimica et Cosmochimica Acta 58 (15), 3281–3287. http://dx.doi.org/10.1016/0016-7037(94)90056-6.

Stern, C.R., Kilian, R., 1996. Role of the subducted slab, mantle wedge and continental crust in the generation of adakites from the Andean Austral volcanic zone. Contrib. Mineral. Petrol. 123 (3), 263–281. http://dx.doi.org/10.1007/s004100050155.

Sugden, D.E., McCulloch, R.D., Bory, A.J.M., Hein, A.S., 2009. Influence of Patagonian glaciers on Antarctic dust deposition during the last glacial period. Nat. Geosci. 2 (4), 281–285. http://dx.doi.org/10.1038/ngeo474.

Tanaka, T., Togashi, S., Kamioka, H., Amakawa, H., Kagami, H., Hamamoto, T., Dragusanu, C., 2000. JNdi-1: a neodymium isotopic reference in consistency with La Jolla neodymium. Chem. Geol. 168 (3–4), 279–281. http://dx.doi.org/10.1016/s0009-2541(00)00198-4.

Tohver, E., D'Agrella-Filho, M.S., Trindade, R.I.F., 2006. Paleomagnetic record of Africa and South America for the 1200-500 Ma interval, and evaluation of Rodinia and Gondwana assemblies. Precambrian Res. 147 (3–4), 193–222. http://dx.doi.org/10.1016/j.precamres.2006.01.015.

Ulke, A.G., Andrade, M.F., 2001. Modeling urban air pollution in São Paulo, Brazil: sensitivity of model predicted concentrations to different turbulence parameterisations. Atmos. Environ. 35 (10), 1747–1763. http://dx.doi.org/10.1016/s1352-2310(00)00498-2.

Weis, D., Kieffer, B., Maerschalk, C., Barling, J., de Jong, J., Williams, G.A., Mahoney, J.B., 2006. High-precision isotopic characterisation of USGS reference materials by TIMS and MC-ICP-MS. Geochem. Geophys. Geosyst. 7. http://dx.doi.org/10.1029/2006gc001283.

Weiss, D.J., Kober, B., Dalgopolova, A., Gallagher, K., Spiro, B., Le Roux, G., Coles, B.J., 2004. Accurate and precise Pb isotope ratio measurements in environmental samples by MC-ICP-MS. Int. J. Mass spectrom. 232 (3), 205–215. http://dx.doi.org/10.1016/j.ijms.2004.01.005.

Witt, M., Baker, A.R., Jickells, T.D., 2006. Atmospheric trace metals over the Atlantic and South Indian Oceans: investigation of metal concentrations and lead isotope ratios in coastal and remote marine aerosols. Atmos. Environ. 40 (28), 5435–5451. http://dx.doi.org/10.1016/j.atmosenv.2006.04.041.

Yu, Z.S., Robinson, P., McGoldrick, P., 2001. An evaluation of methods for the chemical decomposition of geological materials for trace element determination using ICP-MS. Geostandards Newsletter-the J. Geostand. Geoanal. 25 (2–3), 199–217. http://dx.doi.org/10.1111/j.1751-908X.;1;2001.tb00596.x.

Zdanowicz, C., Hall, G., Vaive, J., Amelin, Y., Percival, J., Girard, I., Biscaye, P., Bory, A., 2006. Asian dustfall in the St. Elias mountains, Yukon, Canada. Geochimica et Cosmichimica Acta 70, 3493–3507.